hardware

MDPI

Article

Pressure-Dependent Facial Expression Control Using Calibrated Force-Sensitive Sensors

Naoya Morikawa [1] and Emi Yuda [2,3,*]

1 Department of Information Engineering, Graduate School of Engineering, Mie University, Tsu 514-8507, Japan; 426m532@m.mie-u.ac.jp
2 Innovation Center for Semiconductor and Digital Future, Mie University, Tsu 514-8507, Japan
3 Department of Management Science and Technology, Graduate School of Engineering, Tohoku University, Sendai 980-8579, Japan
* Correspondence: yuda@icsdf.mie-u.ac.jp or emi.a.yuda@tohoku.ac.jp

Abstract

This study presents a compact affective sensing system that converts physical touch into intuitive multimodal feedback through dynamic facial expressions and optional audio responses. The system was developed to support non-verbal, human-centered interaction in embedded human–machine interfaces, where tactile input can be directly associated with emotional perception. The hardware platform is based on the M5Stack CoreS3, integrating a force-sensitive resistor (FSR), an ESP32-S3 microcontroller, an embedded LCD, and a built-in speaker. Pressure signals are acquired using a simple voltage divider circuit and digitized through the built-in 12-bit analog-to-digital converter (ADC) of the ESP32-S3. To improve signal stability, a simple moving average (SMA) filter is applied for noise reduction. The normalized pressure signal is classified into multiple pressure regions and mapped to emotional states. Smooth facial transitions are generated by continuously interpolating geometric facial parameters, including mouth curvature, eye shape, and eyebrow angle, without relying on pre-rendered images. Experimental evaluation demonstrated stable pressure detection, low-latency response, and intuitive emotional feedback across a wide operating range. User evaluation results further indicated that the combination of visual and auditory feedback enhanced realism, anthropomorphic perception, and interaction quality. The proposed system demonstrates the potential of tactile affective sensing for applications in assistive communication, education, and empathetic human–robot interaction systems.

Keywords: affective sensing; force-sensitive resistor (FSR); human–machine interaction; tactile feedback; embedded systems; emotional expression; real-time processing; visual interface

Check for updates

Received: 27 March 2026
Revised: 11 June 2026
Accepted: 12 June 2026
Published: 1 July 2026

1. Introduction

In recent years, human–machine interaction (HMI) has increasingly emphasized intuitive and emotionally expressive interfaces. The concept of affective computing, originally proposed by Rosalind W. Picard, established the theoretical foundation for enabling machines to recognize, interpret, and express human emotions [1]. Building upon this framework, early work by Cynthia Breazeal demonstrated that embedding emotional models into humanoid robots significantly enhances social interaction and user engagement [2]. Subsequent studies on social and expressive robotics further highlighted the importance of emotional feedback in improving empathy, trust, and long-term interaction between humans and machines [3–5].

Despite these advances, many existing affective interaction systems rely on complex multimodal sensing architectures and computationally intensive algorithms, limiting their applicability to compact and low-cost embedded devices. In particular, the conversion of simple tactile stimuli, such as touch and pressure, into intuitive emotional feedback remains insufficiently explored. Tactile interaction is inherently direct, non-verbal, and physically intuitive, making it a promising modality for human-centered interaction systems.

Force-sensitive resistors (FSRs) provide a simple and low-cost approach for detecting pressure-based interaction. Combined with embedded microcontrollers and compact displays, FSR-based systems can support real-time emotional feedback without requiring large-scale computational resources. However, many existing tactile interaction systems rely on predefined images or discrete symbolic indicators, limiting the smoothness and expressiveness of interaction.

To address these limitations, this study proposes a compact pressure-dependent affective sensing system that converts physical touch into dynamic facial expressions in real time. The proposed system is implemented using an M5Stack CoreS3 platform integrating an ESP32-S3 microcontroller, an FSR-based pressure input module, an embedded LCD display, and optional audio feedback. Pressure signals are acquired through a simple voltage divider circuit and processed in real time using lightweight signal conditioning techniques. The normalized pressure values are mapped to emotional states, and facial expressions are generated through procedural geometric rendering based on continuously varying facial parameters such as mouth curvature, eye shape, and eyebrow angle.

Unlike conventional pre-rendered animation approaches, the proposed method enables low-latency and computationally efficient emotional expression generation suitable for embedded systems. Through experimental evaluation and subjective user assessment, this study investigates whether tactile input combined with dynamic visual feedback can improve emotional realism, anthropomorphic perception, and interaction quality. The proposed system contributes to the development of intuitive, low-cost, and human-centric affective interfaces for applications in assistive communication, education, and empathetic human–robot interaction.

2. Device Design

The proposed system was designed as a compact affective sensing platform that converts contact pressure into real-time emotional feedback through dynamic facial expressions. The hardware configuration consists of three primary modules: (i) a pressure input module using a force-sensitive resistor (FSR), (ii) a processing module based on the M5Stack CoreS3 equipped with an ESP32-S3 microcontroller (Espressif Systems (Shanghai) Co., Ltd., Shanghai, China), and (iii) an output module utilizing the integrated LCD display and optional audio feedback through the built-in speaker. The overall design prioritizes low-cost implementation, real-time responsiveness, and ease of integration for embedded human–machine interaction applications.

The pressure input module employs a piezoresistive FSR because of its thin structure (<0.4 mm), fast response time (<10 ms), mechanical flexibility, and low implementation cost. Compared with load cells and capacitive sensing systems, FSRs are easier to integrate into compact embedded devices and are suitable for intuitive touch interaction. However, FSR sensors inherently exhibit nonlinear resistance characteristics and limited absolute force accuracy. Therefore, the present system was designed for relative pressure estimation and emotional interaction rather than precision force measurement.

Pressure signals were acquired using a simple voltage divider circuit consisting of the FSR and a 10 kΩ resistor. The analog voltage output was directly connected to the built-in 12-bit analog-to-digital converter (ADC) of the ESP32-S3 microcontroller without additional operational amplifier circuitry. The digitized signal was processed in real time using a simple moving average (SMA) filter for noise reduction and signal stabilization. The selected SMA window size provided a practical balance between response latency and noise suppression during interactive operation.

The processing module utilizes the ESP32-S3 dual-core microcontroller operating at 240 MHz, enabling simultaneous execution of sensor acquisition and graphical rendering tasks with low latency. Facial expressions were generated using procedural geometric rendering rather than pre-rendered image assets. Specifically, normalized pressure values were mapped to continuously varying facial parameters, including mouth curvature, eye shape, and eyebrow angle. Intermediate pressure values were linearly interpolated between predefined emotional states to produce smooth visual transitions during interaction. The pressure-to-emotion mapping is defined in Table 1 and illustrated in Figure 1.

Table 1. Mapping between pressure levels and corresponding emotional expressions and visual feedback.

Pressure Range (P)	Emotional State	Visual Cue	Meaning of Expression
$0 \leq P < 25\%$	Comfort	Yellow	Smile/Neutral, Positive
$25 \leq P < 50\%$	Slight Discomfort	Green	Caution/Mild Reaction
$50 \leq P < 75\%$	Discomfort	Blue	Serious Expression/Confusion
$75 \leq P \leq 100\%$	Pain	Red	Anger/High Distress

Footer: P denotes the normalized pressure value (%). Emotional states are categorized into four levels based on pressure intensity and are represented through corresponding colors and facial expressions for intuitive real-time feedback.

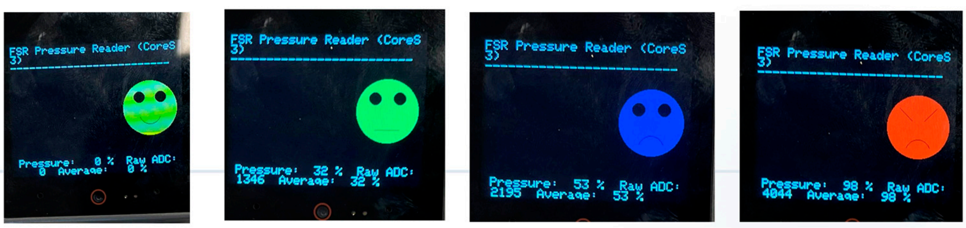

Figure 1. Pressure-Dependent Emotional State Transition and Facial Expression Mapping. The figure illustrates the relationship between normalized pressure input values (P) and the corresponding emotional states generated by the proposed affective sensing system. As the applied pressure increases from left to right, the system transitions through multiple emotional response regions, each associated with different facial expressions, visual feedback patterns, and optional audio responses. The normalized pressure signal is continuously processed and mapped to predefined emotional states using threshold-based classification combined with linear interpolation between adjacent states. This interpolation enables smooth transitions in facial parameters, including mouth curvature, eye shape, and eyebrow angle, rather than abrupt switching between discrete expressions. The figure additionally summarizes how increasing pressure intensity influences the perceived emotional response and interaction feedback presented on the embedded LCD display.

The integrated 320 × 240 pixel IPS LCD provides sufficient resolution and viewing angle for expressive visualization while reducing wiring complexity compared with external display modules. Optional audio feedback was additionally implemented using the built-in speaker of the M5Stack CoreS3 to enhance emotional interaction during experimental demonstrations.

From a cost perspective, the system was designed as a low-cost embedded platform suitable for scalable deployment and educational prototyping. The approximate hardware cost consisted of the M5Stack CoreS3 module (USD 40–60), the FSR sensor (approximately USD 12), and passive electronic components (<USD 5), resulting in a total estimated cost below USD 80.

Recent advances in pressure sensing technologies, including microelectromechanical systems (MEMS), flexible capacitive sensors, and bio-inspired electronic skin, have demonstrated remarkable improvements in sensitivity, spatial resolution, and mechanical robustness [6–11]. Although these advanced sensing systems provide high accuracy and sophisticated tactile perception capabilities, they often require complex fabrication processes, multilayer structures, or specialized materials, limiting their applicability in compact and low-cost embedded systems. In contrast, the present study adopted a pragmatic design strategy emphasizing simplicity, affordability, and rapid implementation while maintaining sufficient responsiveness for real-time affective interaction.

Overall, the proposed device architecture demonstrates a practical trade-off between sensing precision and system simplicity. Although the use of an FSR limits quantitative force accuracy, the system effectively achieves its primary objective of intuitive pressure-dependent emotional feedback for compact human-centered interaction systems. The hardware components used in this study are summarized in Table 2.

Table 2. Bill of Materials.

Quantity	Component	Material Type (Category)	Specifications & Features	Source of Materials	Material Type (Major Materials)	Cost (Approx.)
1	M5Stack CoreS3	Embedded Controller	• Dual-core ESP32-S3 processor • Built-in camera, MIC, and Speaker • 2.0-inch IPS LCD touch screen • Integrated 6-axis IMU (BMI270)	Switch Science (https://www.switch-science.com/products/8960, accessed on 1 March 2026)	ABS Plastic/FR-4 PCB	$40–60
1	Pressure Sensor (FSR 406)	Force Sensor	• Force Sensitive Resistor (FSR) • Sensing range: 0.1 N to 100 N • Sensing area: 38.1 × 38.1 mm square • Ultra-thin (0.45 mm thickness)	Akizuki Denshi (https://akizukidenshi.com/catalog/g/g116089/, accessed on 1 March 2026)	Polyimide (Kapton) Film	$12.00
1	Carbon Film Resistor (10 kΩ)	Passive Component	• Resistance: 10k Ohm • Power rating: 1/6 W (0.166 W) • Tolerance: ±5% • Used as a pull-down/voltage divider	Akizuki Denshi (https://akizukidenshi.com/catalog/g/g116103/, accessed on 1 March 2026)	Carbon/Ceramic	$0.10

https://doi.org/10.3390/hardware4030013

Table 2. *Cont.*

Quantity	Component	Material Type (Category)	Specifications & Features	Source of Materials	Material Type (Major Materials)	Cost (Approx.)
1	Breadboard (EIC-801)	Prototyping Board	• 400 tie-points (Total) • 2 Power rails with adhesive back • Standard 0.1″ (2.54 mm) pitch • Size: 82 × 53 × 8.5 mm	Switch Science (https://www.switch-science.com/products/313, accessed on 1 March 2026)	ABS Plastic/Nickel-Silver	$3.00
1	Jumper Wire Set (10 pcs)	Interconnects	• Male-to-Male (M-M) type • Multiple colors for easy wiring • Length: approx. 200 mm • Flexible stranded copper wire	Switch Science (https://www.switch-science.com/products/209, accessed on 1 March 2026)	PVC Insulation/Copper	$2.50

This setup utilizes the M5Stack CoreS3 as the main controller to acquire data from the FSR 406 pressure sensor. The 10 kΩ resistor is required to form a voltage divider circuit with the FSR to convert force into an analog voltage signal. Data can be processed via the CoreS3's ESP32-S3 chip and displayed on the LCD or transmitted via Wi-Fi/Bluetooth for bio-signal analysis. The Breadboard and Jumper Wires facilitate rapid prototyping without soldering, which is ideal for undergraduate (B4) student experiments. The Material type (Category) indicates the function of the device (controller, sensor, etc.). The Material type (Major Materials) indicates the chemical constituent materials (plastic, substrate, film, etc.) and is described with environmental regulations (RoHS, etc.) in mind. The total amount is $77.60.

3. Build Instructions

This section describes the procedure for constructing the proposed pressure-dependent affective sensing system. The system was designed as a compact and low-cost embedded platform that converts tactile pressure input into real-time emotional feedback through dynamic facial expressions and optional audio responses. The implementation assumes basic familiarity with embedded electronics, voltage divider circuits, and microcontroller programming.

3.1. Required Components

The hardware configuration consists of the following components:

- M5Stack CoreS3 (ESP32-S3 microcontroller with integrated LCD and speaker);
- Force-Sensitive Resistor (FSR);
- Fixed resistor (10 kΩ);
- Jumper wires;
- Breadboard or printed circuit board (PCB);
- USB Type-C cable for power supply and programming.

Optional components include an enclosure case, adhesive materials for sensor mounting, and a compliant silicone layer for pressure stabilization.

3.2. Input Circuit Configuration

The pressure sensing module was implemented using a simple voltage divider circuit consisting of the FSR and a 10 kΩ resistor. One terminal of the FSR was connected to the 3.3 V supply, while the opposite terminal was connected simultaneously to the analog input pin and the fixed resistor. The remaining resistor terminal was connected to ground (GND). The analog voltage generated by the divider circuit was directly digitized using the built-in 12-bit ADC of the ESP32-S3 microcontroller without additional operational amplifier circuitry (Figure 2).

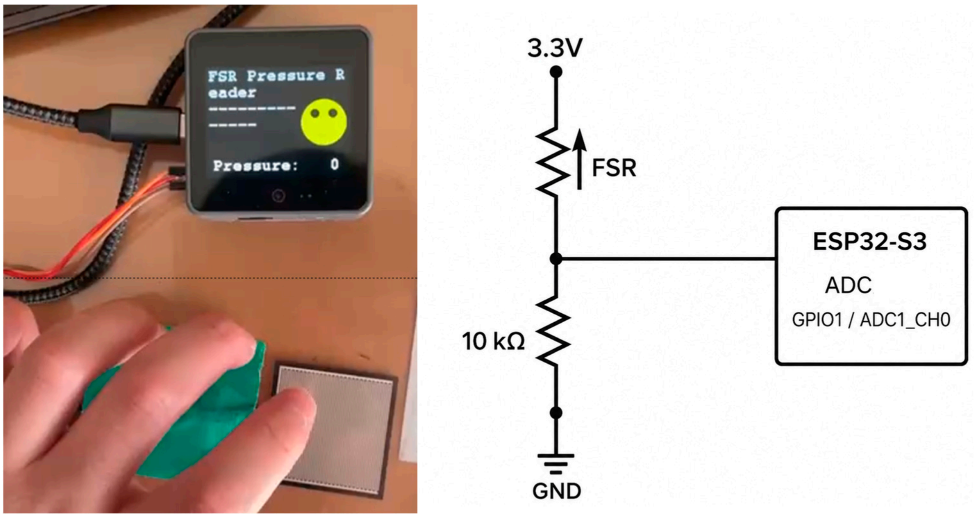

(**a**) (**b**)

Figure 2. Overall System Configuration and Pressure Signal Acquisition Circuit. (**a**) Overview of the proposed affective sensing system implemented on the M5Stack CoreS3 platform. The system consists of a force-sensitive resistor (FSR) input module, an ESP32-S3 microcontroller for real-time signal processing, an integrated LCD for facial expression rendering, and an optional built-in speaker for supplementary audio feedback. Pressure input applied to the FSR is converted into emotional feedback through dynamic facial expression generation. (**b**) Circuit configuration of the pressure sensing module based on a simple voltage divider. The FSR and a 10 kΩ fixed resistor are connected between the 3.3 V supply and ground (GND), and the intermediate voltage is directly connected to the ADC input pin (GPIO1/ADC1_CH0) of the ESP32-S3. Variations in applied pressure change the FSR resistance, producing corresponding voltage changes that are digitized using the built-in 12-bit analog-to-digital converter (ADC). No operational amplifier circuitry was used in the final implementation.

In the present implementation, the FSR output was connected to GPIO1 (ADC1_CH0) of the ESP32-S3. The selected resistor value provided a practical compromise between sensitivity and dynamic range for interactive pressure detection. Alternative resistor values may be used depending on the target pressure range and sensitivity requirements.

3.3. Mechanical Sensor Mounting

The FSR was attached to a flat surface using adhesive tape or a thin protective layer to maintain stable pressure distribution during interaction. Rigid mounting materials were avoided because they may produce localized stress concentration and unstable sensor response. In some experiments, a compliant silicone sheet was additionally placed above the sensor surface to improve force uniformity and tactile consistency.

3.4. Firmware and Signal Processing

The firmware was implemented using the Arduino IDE environment for the ESP32-S3 platform. The processing flow consisted of the following steps:

(1) Initialization of the 12-bit ADC module;
(2) Acquisition of analog pressure signals from the FSR circuit;
(3) Application of a Simple Moving Average (SMA) filter for noise reduction;
(4) Signal normalization into a relative pressure scale;

(5) Mapping of normalized pressure values to emotional states;
(6) Real-time rendering of facial expressions and optional audio feedback.

To stabilize sensor fluctuations while maintaining low latency, an SMA filter with a window size of 5 samples was applied in the validation experiments.

3.5. Real-Time Facial Rendering

Facial expressions were generated procedurally on the integrated LCD display rather than using pre-rendered bitmap images. The rendering process dynamically modified geometric facial parameters according to the normalized pressure input.

Specifically:

- Eye shapes were generated using parameterized circular geometries;
- Mouth curvature was continuously adjusted using arc-based functions;
- Eyebrow angles were modified according to emotional state intensity;
- Background color was dynamically varied to enhance emotional expression.

Intermediate pressure values were linearly interpolated between predefined emotional states, enabling smooth transitions rather than abrupt discrete switching. This rendering strategy minimized memory consumption and reduced computational overhead while maintaining low-latency visual feedback.

3.6. Signal Normalization and Threshold Adjustment

Because FSR sensors exhibit nonlinear resistance characteristics and device-to-device variability, a simple signal normalization procedure was performed prior to use. Representative pressure inputs, including light touch, moderate press, and strong press, were applied to determine practical threshold ranges for emotional state mapping. The system was designed for relative pressure interaction rather than absolute force calibration.

3.7. Design Considerations

The proposed architecture emphasizes simplicity, low cost, and ease of implementation for embedded affective interaction systems.

- The FSR sensor was selected because of its flexibility, low cost, and ease of integration, although higher-precision alternatives such as capacitive or piezoelectric sensors are available.
- The ESP32-S3 platform provided sufficient computational capability for simultaneous signal processing and graphical rendering.
- The integrated LCD reduced wiring complexity and improved hardware robustness compared with external display modules.

This pragmatic configuration enables rapid prototyping and scalable deployment in educational and human–machine interaction applications.

3.8. Visual References

The manuscript includes the following visual materials:

- Circuit schematic of the FSR voltage divider;
- System block diagram illustrating signal flow;
- Examples of facial expression transitions under different pressure conditions period

3.9. Safety Considerations

The following precautions should be considered during system construction and operation:

- Ensure operation within the 3.3 V input range of the ESP32-S3;

- Avoid excessive force beyond the rated operating range of the FSR;
- Use insulated wiring to prevent electrical short circuits;
- Ensure adequate heat dissipation when the device is enclosed.

Following these procedures, the proposed system can be reliably reproduced as a compact and low-cost platform for pressure-based emotional interaction research.

4. Operating Instructions

This section describes the operational procedure of the proposed pressure-dependent affective sensing system. The system was designed to provide stable and intuitive real-time interaction by converting tactile pressure input into dynamic facial expressions and optional audio feedback.

4.1. System Initialization

The M5Stack CoreS3 was powered through a USB Type-C connection using a regulated 5 V power source supplied either by a personal computer or an external adapter. After power-on, the firmware automatically initialized the ADC module, LCD display, and rendering engine. A neutral facial expression representing the baseline emotional state appeared on the display within approximately 1–2 s.

Before operation, the user confirmed that the FSR module was correctly connected to the designated ADC input pin (GPIO1/ADC1_CH0). If no pressure input was detected, the system remained in the neutral state.

4.2. Pressure Interaction and Real-Time Feedback

During operation, pressure was applied to the FSR surface using a fingertip or a soft object. Concentrated mechanical stress, such as sharp fingernail contact, was avoided to prevent sensor damage and unstable force distribution.

The system continuously acquired analog pressure signals through the built-in 12-bit ADC of the ESP32-S3. The acquired signal was filtered using a Simple Moving Average (SMA) filter with a window size of 5 samples to reduce electrical noise while maintaining low-latency response characteristics.

The normalized pressure value was mapped to emotional states associated with dynamically generated facial expressions. Lower pressure levels produced neutral or relaxed expressions, whereas increasing pressure gradually generated discomfort- and pain-related facial responses. Rather than abrupt switching between discrete states, intermediate pressure values were linearly interpolated to continuously modify facial parameters such as mouth curvature, eye geometry, eyebrow angle, and background color intensity.

The response time of the sensing system was below approximately 10 ms under standard operating conditions, enabling visually continuous real-time interaction without perceptible delay.

4.3. Operational Signal Calibration and Threshold Setting

Because FSR sensors exhibit nonlinear response characteristics and device-to-device variability, a practical signal normalization procedure was performed before operation. The baseline signal level was automatically measured immediately after startup under no-contact conditions to reduce the influence of electrical noise and sensor drift.

Representative pressure inputs, including light touch, moderate press, and strong press, were subsequently applied to determine practical threshold ranges for emotional state mapping. These threshold values could be adjusted within the firmware depending on the intended interaction sensitivity and operating environment.

https://doi.org/10.3390/hardware4030013

The SMA filter window size and threshold parameters were additionally configurable to balance noise suppression, responsiveness, and emotional transition smoothness.

4.4. Facial Expression Generation Logic

The internal signal processing flow of the proposed system is summarized as follows:

Pressure Input → ADC Conversion → SMA Filtering → Signal Normalization → Emotional State Mapping → Procedural Facial Rendering.

Facial expressions were generated procedurally rather than using bitmap image assets. Geometric facial parameters, including mouth curvature, eye shape, and eyebrow angle, continuously varied according to the normalized pressure signal. This rendering strategy minimized memory usage and enabled computationally efficient low-latency visualization on the embedded platform.

Optional audio feedback synchronized with emotional states was additionally implemented through the built-in speaker to enhance interaction realism during experimental demonstrations.

4.5. Operational Safety Guidelines

To ensure stable operation and prevent hardware damage, several precautions were considered during system use.

Mechanical Considerations:

- Excessive force beyond the rated operating range of the FSR was avoided.
- Excessive bending or folding of the sensor substrate was prevented.

Electrical Considerations:

- Only regulated 5 V power sources were used.
- Short circuits between GPIO pins and power lines were avoided.

Thermal Considerations:

- Prolonged operation in high-temperature environments (>50 °C) was avoided to maintain stable sensor and microcontroller performance.

Usage Limitations:

- The proposed system was developed for affective interaction research and educational purposes.
- The displayed emotional responses should not be interpreted as clinical pain measurements or medical diagnostic indicators.

4.6. Troubleshooting

Table 3 summarizes representative operational issues, possible causes, and recommended corrective actions for the proposed system.

Table 3. Troubleshooting guide for the pressure-dependent affective sensing system.

Issue	Possible Cause	Recommended Solution
No display output	Power supply issue	Verify USB connection and power source
No pressure response	FSR wiring disconnection	Confirm sensor wiring and ADC pin connection
Unstable or noisy signal	Electrical noise or unstable contact	Increase SMA filter window size or stabilize sensor mounting
Saturated signal output	Improper threshold adjustment	Modify normalization range and threshold parameters
Delayed facial response	Excessive filtering parameters	Reduce SMA window size

https://doi.org/10.3390/hardware4030013

Users were encouraged to verify wiring conditions, threshold settings, and power stability before performing advanced troubleshooting procedures.

4.7. System Shutdown

The system could be powered off by disconnecting the USB Type-C cable. No dedicated shutdown sequence was required because all processing operations were executed in volatile memory. Overall, the proposed operating procedure enabled stable and intuitive real-time mapping between tactile pressure input and dynamic emotional feedback while maintaining low hardware complexity and low computational cost.

5. Validation

To evaluate the effectiveness of the proposed pressure-dependent affective sensing system, quantitative and qualitative experiments were conducted focusing on pressure response characteristics, real-time responsiveness, emotional mapping validity, and system stability during continuous interaction.

5.1. Pressure–Response Characterization

A controlled loading experiment was conducted using reference weights ranging from 20 g to 5 kg. Incremental loads were applied to the FSR sensor, and the corresponding ADC output values (0–4095) were recorded through the built-in 12-bit ADC of the ESP32-S3 microcontroller. Each loading condition was repeated 10 times to evaluate repeatability.

The measured sensor output increased monotonically with increasing applied force over the operating range. As expected for piezoresistive FSR devices, the sensor response exhibited nonlinear characteristics, particularly in the low-pressure region. Therefore, the proposed system utilized relative signal normalization and threshold-based emotional mapping rather than absolute force estimation.

Repeatability analysis demonstrated that the coefficient of variation remained below 5% within the intermediate operating range (0.5–3 kg), indicating stable response characteristics suitable for interactive affective feedback applications. Error bars representing standard deviation are additionally included in the experimental plots to visualize signal variability across repeated measurements.

5.2. Real-Time Response Performance

The temporal response performance of the system was evaluated by measuring the delay between pressure application and visual update on the LCD display. End-to-end latency was estimated using high-speed video analysis synchronized with the pressure input event.

The measured total system latency, including sensor acquisition, signal filtering, emotional state mapping, and facial rendering, remained below approximately 15 ms under standard operating conditions. This latency level satisfies typical real-time interaction requirements for human–machine interfaces, where delays greater than approximately 50 ms may reduce the perception of immediacy and responsiveness.

The use of procedural geometric rendering additionally reduced memory access overhead and contributed to stable low-latency operation on the embedded platform.

5.3. Validation of Emotional State Mapping

To evaluate the perceptual validity of the proposed emotional feedback system, a subjective user study was conducted with 12 participants. Participants were instructed to apply three levels of pressure intensity (low, medium, and high) to the FSR sensor and evaluate whether the displayed facial expression appropriately reflected their perceived interaction intensity.

The proposed system achieved a mean agreement rate of 91.7% across all participants. Misclassification events occurred primarily between adjacent pressure levels, particularly between medium- and high-intensity conditions, suggesting that the emotional transition boundaries were generally intuitive and perceptually consistent.

To improve statistical interpretability, the 95% confidence interval of the agreement rate was additionally calculated. The results support the reliability of the proposed pressure-to-emotion mapping strategy for intuitive affective interaction.

Furthermore, subjective evaluation results indicated that the combination of dynamic facial rendering and optional audio feedback enhanced perceived realism, anthropomorphic impression, and interaction quality during operation.

5.4. Comparison with Reference Force Measurement

To evaluate relative sensing reliability, the proposed FSR-based system was compared with a commercial load cell measurement setup under identical loading conditions. The normalized FSR output demonstrated a strong positive correlation with the reference force measurements.

The Pearson correlation coefficient between normalized FSR output and reference force values was $r = 0.93$ ($p < 0.001$). This result indicates that, although the FSR sensor does not provide high-precision force measurement comparable to laboratory-grade load cells, it reliably captures relative pressure variation suitable for expressive interaction and emotional feedback applications.

5.5. Long-Term System Stability

The integrated sensing–processing–rendering pipeline was evaluated during continuous interaction sessions lasting approximately 60 min. Throughout the experiment, the system maintained stable operation without noticeable signal drift, rendering instability, or response delay accumulation.

No significant degradation in sensor response or visualization quality was observed during prolonged operation, confirming the robustness of the embedded implementation for continuous interactive use.

5.6. Summary of Validation Results

The experimental results demonstrated that the proposed system:

- Reliably detected pressure-dependent interaction signals;
- Provided low-latency real-time emotional feedback;
- Achieved high perceptual agreement between pressure intensity and displayed facial expressions;
- Maintained stable operation during prolonged interaction;
- Successfully balanced implementation simplicity, low cost, and intuitive affective interaction capability.

Overall, the proposed device effectively fulfilled its intended objective as a compact pressure-dependent affective sensing interface for embedded human–machine interaction applications.

6. Discussion

Recent advances in pressure sensing and tactile interaction technologies have significantly expanded the applicability of contact-based human–machine interfaces. In particular, pressure image sensing and body-contact analysis have recently attracted considerable attention in ubiquitous computing, healthcare monitoring, and human-centered sensing applications. Previous studies have demonstrated the effectiveness of pressure sensor

https://doi.org/10.3390/hardware4030013

matrices for evaluating sensing characteristics and sampling strategies, as well as for reconstructing human posture and body shape from contact pressure distributions [12–18]. For example, pressure-image-based approaches have been applied to in-bed posture reconstruction, smart-chair human pose estimation, and body-weight estimation using deep learning techniques. These studies primarily focus on spatial pressure analysis and quantitative biomechanical estimation using high-density sensing architectures.

Compared with these approaches, the present study adopts a fundamentally different design objective. Rather than reconstructing detailed body geometry or estimating biomechanical parameters, the proposed system focuses on intuitive affective interaction by transforming simple tactile pressure input into emotional visual feedback. This design philosophy prioritizes immediacy, interpretability, and low computational complexity over high-resolution pressure imaging.

Recent multimodal tactile sensing research has additionally demonstrated the importance of combining pressure information with other sensing modalities, including inertial sensing, smart textiles, and body-centered interaction systems [19–21]. Such multimodal approaches enable more robust motion estimation, user identification, and context-aware interaction. Inspired by these developments, the proposed system incorporates not only pressure sensing but also multimodal emotional feedback through dynamic facial rendering and optional audio output. Although the present implementation remains intentionally lightweight, future extensions may integrate additional physiological and motion-based sensing modalities to improve emotional expressiveness and adaptive interaction capability.

From the perspective of affective computing and emotional interaction research, substantial progress has been achieved in facial expression recognition, emotion estimation, and human–robot interaction systems [22–31]. Previous studies have explored transformer-based facial expression recognition, self-supervised facial dynamics analysis, group emotion recognition, emotional voice conversion, and pain estimation using facial motion analysis. These approaches generally rely on large-scale datasets, machine learning models, and high computational resources to infer emotional states from human behavior.

In contrast, the present study approaches affective interaction from the opposite direction: rather than recognizing human emotion, the proposed system generates emotional expressions directly from tactile interaction input. This "pressure-to-emotion" mapping strategy represents a lightweight affective interface suitable for embedded real-time applications. Furthermore, unlike conventional bitmap-based emotional interfaces, the proposed procedural rendering method continuously modifies geometric facial parameters according to normalized pressure intensity, enabling smooth low-latency emotional transitions while minimizing memory consumption.

The proposed work therefore exists at the intersection of three emerging research domains:

(1) Pressure sensing and tactile interaction systems;
(2) Affective visualization and emotional human–machine interaction;
(3) Low-cost real-time embedded interface design.

This interdisciplinary positioning represents one of the primary contributions of the study. While the sensing accuracy of the FSR-based system is lower than that of advanced MEMS or pressure imaging technologies, the proposed architecture demonstrates that intuitive emotional interaction can still be achieved using simple, inexpensive, and computationally lightweight hardware.

Several limitations should nevertheless be acknowledged. First, the current system relies on a single-point FSR input and therefore cannot capture detailed spatial pressure distributions. Second, emotional state mapping was implemented using threshold-based normalization and linear interpolation rather than adaptive learning models. Third, the user

https://doi.org/10.3390/hardware4030013

validation study was conducted with a relatively small number of participants and focused primarily on perceptual agreement rather than long-term usability or psychological effects. In addition, the present implementation evaluated only a limited number of emotional states and interaction scenarios.

Future work may therefore focus on integrating high-resolution pressure sensing arrays, multimodal physiological signals, and adaptive machine learning algorithms to improve emotional representation capability and personalization. Advanced sensing technologies such as capacitive tactile sensors, MEMS-based pressure sensors, or flexible electronic skin may further improve sensitivity and durability. Moreover, combining pressure sensing with physiological signals such as heart rate variability, respiration, or motion sensing could enable richer context-aware affective interaction.

Another promising direction involves extending the proposed framework toward wearable systems, assistive communication devices, and empathetic robotic platforms. Real-time tactile affective feedback may contribute to inclusive human–machine interfaces for education, rehabilitation, social robotics, and emotionally adaptive environments.

7. Conclusions

This study presented the design, implementation, and validation of a compact pressure-dependent affective sensing system that converts tactile pressure input into dynamic emotional feedback through procedural facial expression rendering. The proposed system successfully demonstrated that intuitive emotional interaction can be achieved using a low-cost embedded platform composed of a force-sensitive resistor (FSR), an ESP32-S3 microcontroller, and an integrated LCD interface.

Experimental evaluations confirmed stable pressure detection, low-latency real-time responsiveness, and strong correlation with reference force measurements. Subjective user evaluations additionally demonstrated high perceptual agreement between applied pressure intensity and displayed emotional expressions. The results indicate that the proposed system effectively supports intuitive human-centered interaction despite the inherent nonlinearity and limited quantitative accuracy of FSR sensors.

A major contribution of this work lies in the practical balance achieved between implementation simplicity, computational efficiency, and affective expressiveness. Unlike many existing affective computing systems that require complex multimodal sensing architectures or computationally intensive machine learning models, the proposed system utilizes lightweight procedural rendering and threshold-based emotional mapping suitable for compact embedded devices.

The study further demonstrated that tactile input can serve as an effective modality for intuitive emotional interaction in low-cost human–machine interfaces. By combining pressure sensing, real-time signal processing, and dynamic facial visualization, the proposed architecture contributes to the growing field of embedded affective interaction systems.

Future research may focus on expanding the emotional representation capability through multimodal sensing, adaptive algorithms, and high-resolution tactile sensing technologies. Integration with wearable devices, robotic systems, and physiological monitoring platforms may further enable empathetic and context-aware interaction systems for healthcare, education, rehabilitation, and social robotics applications.

Overall, the proposed system provides a practical and scalable framework for pressure-based affective interaction, demonstrating the feasibility of translating tactile stimuli into intuitive emotional feedback using compact real-time embedded hardware.

Supplementary Materials: The following supporting information can be downloaded at: https://www.mdpi.com/article/10.3390/hardware4030013/s1.

Name	Type	Description
M5CoreS3-FSR	Arduino sketch file (.ino)	A source code file used in the Arduino development environment to write, compile, and upload programs to microcontroller boards. It typically contains setup and loop functions that define the device behavior.
pain	Audio (.wav)	Audio files that are played when a pressure sensor is pressed, triggering voice outputs as "It hurts".
ouch	Audio (.wav)	Audio files that are played when a pressure sensor is pressed, triggering voice outputs as "That tickles".

Key Technical Details: Logic Integration: The .ino file acts as the "brain," linking the hardware input (FSR sensor) to the software output (playing the .wav files). Audio Format: The .wav format is used to ensure high-quality, uncompressed audio playback, which is standard for microcontrollers like the M5CoreS3 that use I2S or internal DACs for sound. Trigger Mechanism: The code likely monitors the analog value from the FSR; once it exceeds a predefined limit, it calls the corresponding audio file from the SD card or internal memory.

Author Contributions: Conceptualization, N.M. and E.Y.; methodology, N.M.; software, N.M.; validation, N.M. and E.Y.; formal analysis, N.M.; investigation, N.M.; resources, N.M.; data curation, N.M.; writing—original draft preparation, N.M.; writing—review and editing, N.M. and E.Y.; visualization, N.M.; supervision, E.Y.; project administration, E.Y.; funding acquisition, E.Y. All authors have read and agreed to the published version of the manuscript.

Funding: This research was funded by the New Energy and Industrial Technology Development Organization (NEDO), Young Researcher Development Support Project.

Institutional Review Board Statement: Not applicable.

Informed Consent Statement: Not applicable.

Data Availability Statement: The original contributions presented in this study are included in the article/Supplementary Material. Further inquiries can be directed to the corresponding author.

Acknowledgments: During the preparation of this manuscript, the authors used DeepL for the purposes of Translation support. The authors have reviewed and edited the output and take full responsibility for the content of this publication.

Conflicts of Interest: The authors declare no conflicts of interest.

References

1. Picard, R.W. Affective Computing: Challenges. *Int. J. Hum. Comput. Stud.* **2003**, *59*, 55–64. [CrossRef]
2. Breazeal, C. Emotion and Sociable Humanoid Robots. *Int. J. Hum. Comput. Stud.* **2003**, *59*, 119–155. [CrossRef]
3. Leite, I.; Martinho, C.; Paiva, A. Social Robots for Long-Term Interaction: A Survey. *Int. J. Soc. Robot.* **2013**, *5*, 291–308. [CrossRef]
4. Cárdenas, P.; García, J.; Begazo, R.; Aguilera, A.; Dongo, I.; Cardinale, Y. Evaluation of Robot Emotion Expressions for Human–Robot Interaction. *Int. J. Soc. Robot.* **2024**, *16*, 2019–2041. [CrossRef]
5. Savery, R.; Weinberg, G. A Survey of Robotics and Emotion: Classifications and Models of Emotional Interaction. *arXiv* **2023**, arXiv:2007.14838. [CrossRef]
6. Han, X.; Huang, M.; Wu, Z.; Gao, Y.; Xia, Y.; Yang, P.; Fan, S.; Lu, X.; Yang, X.; Liang, L.; et al. Advances in High-Performance MEMS Pressure Sensors: Design, Fabrication, and Packaging. *Microsyst. Nanoeng.* **2023**, *9*, 156. [CrossRef] [PubMed]
7. Huang, H.; Ran, X.; Wan, S.; Wang, Y.; Bi, H. A Flexible Capacitive Pressure Sensor with a Hybrid Porous PDMS/SA Hydrogel Structure for Touch/Pain Detection. *Nanoscale* **2024**, *16*, 17926–17933. [CrossRef] [PubMed]
8. Huang, L.; Tang, Y.; Zhang, P.; Li, Y.; Liu, G.; Zhang, Z.; Zhang, Y.; Yang, R. Flexible Planar Dual-Mode Capacitive Sensor Based on Interdigital Electrodes with Vertical Conductive Ridges for Human–Computer Interaction. *Chem. Eng. J.* **2025**, *520*, 165659. [CrossRef]

9. Fan, Z.; Zhang, L.; Tan, Q.; Yao, X.; Lin, B.; Wang, Y.; Xiong, J. Wearable pressure sensor based on MXene/single-wall carbon nanotube film with crumpled structure for broad-range measurements. *Smart Mater. Struct.* **2021**, *30*, 035024. [CrossRef]
10. Shao, Q.; Yang, G.; Jia, J.; Ma, L. A sensitivity enhanced touch mode capacitive pressure sensor with double cavities. *Microsyst. Technol.* **2023**, *29*, 755–762. [CrossRef]
11. Yoshimoto, S.; Sakamoto, K.; Takeda, R.; Yamamoto, A. Design of a High-Performance Tomographic Tactile Sensor by Manipulating the Detector Conductivity. *IEEE Trans. Ind. Electron.* **2024**, *71*, 16783–16791. [CrossRef]
12. Zhang, Y.; Li, H.; Wang, X. Where to Improve? A Systematic Evaluation of Sampling Parameters for Pressure Sensor Matrix. *Proc. ACM Interact. Mob. Wearable Ubiquitous Technol.* **2025**, *9*, 1–26. [CrossRef]
13. Chen, L.; Xu, M.; Zhao, Y. PI-HMR: Towards Robust In-bed Temporal Human Shape Reconstruction with Contact Pressure Sensing. In Proceedings of the 2025 IEEE/CVF Conference on Computer Vision and Pattern Recognition (CVPR), Nashville, TN, USA, 10–17 June 2025. [CrossRef]
14. Liu, Q.; Sun, J.; Wang, T. In-bed Pressure Image-supported Diffusion for 3D Human Mesh Recovery. In Proceedings of the 2025 IEEE International Conference on Pervasive Computing and Communications (PerCom), Washington, DC, USA, 17–21 March 2025. [CrossRef]
15. Kim, S.; Park, J.; Lee, D. Seeing through the Tactile: 3D Human Shape Estimation from Temporal In-Bed Pressure Images. *Proc. ACM Interact. Mob. Wearable Ubiquitous Technol.* **2024**, *8*, 1–39. [CrossRef]
16. Ke, Y.; Wan, Q.; Xie, F.; Zhen, L.; Wu, Z.; Cai, X. Pressure distribution based 2D in-bed keypoint prediction under interfered scenes. *Pervasive Mob. Comput.* **2024**, *105*, 101979. [CrossRef]
17. Zhao, M.; Xie, F.; Liang, Z.; Cai, X. 3D Human Pose Estimation Using Pressure Images on a Smart Chair. In *Proceedings of the 2024 2nd Asia Conference on Computer Vision, Image Processing and Pattern Recognition (CVIPPR 2024)*; ACM: New York, NY, USA, 2024; pp. 1–6. [CrossRef]
18. Wu, Z.; Wan, Q.; Zhao, M.; Xie, F.; Liang, Z.; Cai, X. MassNet: A Deep Learning Approach for Body Weight Extraction from A Single Pressure Image. In *Proceedings of the 2023 IEEE International Conference on Pervasive Computing and Communications (PerCom)*; IEEE: Piscataway, NJ, USA, 2023; pp. 200–208. [CrossRef]
19. Ying, Q.; Cao, Z.; Wu, Z.; Deng, W.; Zhong, Y.; Diao, Y.; Cai, X. FoRM: Foot-driven Reconstruction of Human Motion Using Dual-Modal Plantar Pressure and Inertial Sensing. *Proc. ACM Interact. Mob. Wearable Ubiquitous Technol.* **2025**, *9*, 1–14. [CrossRef]
20. Zhang, Y.; Wu, Z.; Zhen, L.; Xie, F. Contrastive Learning-Based User Identification with Limited Data on Smart Textiles. *arXiv* **2024**, arXiv:2409.07488. [CrossRef]
21. Reinersmann, A.; Heinz-Jakobs, M.; Röcker, C. Inclusive HCI: Developing Digital Technologies for Supporting Societal Inclusion of Disadvantaged Groups. In *Proceedings of the 35th Australian Computer-Human Interaction Conference (OzCHI '23)*; ACM: New York, NY, USA, 2023; pp. 698–700. [CrossRef]
22. Safavi, F.; Patel, K.; Vinjamuri, R. Facial Expression Recognition with an Efficient Mix Transformer for Affective Human-Robot Interaction. *IEEE Trans. Affect. Comput.* **2025**, *16*, 3081–3094. [CrossRef]
23. Song, S.; Jaiswal, S.; Sanchez, E.; Tzimiropoulos, G.; Shen, L.; Valstar, M. Self-Supervised Learning of Person-Specific Facial Dynamics for Automatic Personality Recognition. *IEEE Trans. Affect. Comput.* **2021**, *14*, 178–195. [CrossRef]
24. Veltmeijer, E.A.; Gerritsen, C.; Hindriks, K.V. Automatic Emotion Recognition for Groups: A Review. *IEEE Trans. Affect. Comput.* **2023**, *14*, 89–107. [CrossRef]
25. Zhou, K.; Sisman, B.; Rana, R.; Schuller, B.W.; Li, H. Emotion Intensity and its Control for Emotional Voice Conversion. *IEEE Trans. Affect. Comput.* **2023**, *14*, 31–48. [CrossRef]
26. Deng, J.; Ren, F. A Survey of Textual Emotion Recognition and Its Challenges. *IEEE Trans. Affect. Comput.* **2023**, *14*, 49–67. [CrossRef]
27. Panda, R.; Malheiro, R.; Paiva, R.P. Audio Features for Music Emotion Recognition: A Survey. *IEEE Trans. Affect. Comput.* **2023**, *14*, 68–88. [CrossRef]
28. Zamzmi, G.; Pai, C.Y.; Goldgof, D.; Kasturi, R.; Ashmeade, T.; Sun, Y. A Comprehensive and Context-Sensitive Neonatal Pain Assessment Using Computer Vision. *IEEE Trans. Affect. Comput.* **2022**, *13*, 28–45. [CrossRef]
29. Allaert, B.; Bilasco, I.M.; Djeraba, C. Micro and Macro Facial Expression Recognition Using Advanced Local Motion Patterns. *IEEE Trans. Affect. Comput.* **2022**, *13*, 147–158. [CrossRef]
30. Baddar, W.J.; Lee, S.; Ro, Y.M. On-the-Fly Facial Expression Prediction Using LSTM Encoded Appearance-Suppressed Dynamics. *IEEE Trans. Affect. Comput.* **2022**, *13*, 159–174. [CrossRef]
31. Chen, Z.; Ansari, R.; Wilkie, D.J. Learning Pain from Action Unit Combinations: A Weakly Supervised Approach via Multiple Instance Learning. *IEEE Trans. Affect. Comput.* **2022**, *13*, 135–146. [CrossRef] [PubMed]

https://doi.org/10.3390/hardware4030013